

Unified intermediate coupling description of the pseudogap and the strange metal phases of cuprates

H. C. Kao,^{*} Dingping Li,[†] and Baruch Rosenstein[‡]
(Dated: August 23, 2022)

A one band Hubbard model with intermediate coupling is shown to describe the two most important unusual features of a normal state: linear resistivity strange metal and the pseudogap. Both the spectroscopic and transport properties of the cuprates are considered on the same footing by employing a relatively simple postgaussian approximation valid for the intermediate couplings $U/t = 1.5 - 4$ in relevant temperatures $T > 100\text{K}$. In the doping range $p = 0.1 - 0.3$, the value of U is smaller than that in the parent material. For a smaller doping, especially in the Mott insulator phase, the coupling is large compared to the effective tight binding scale and a different method is required. This scenario provides an alternative to the paradigm that the coupling should be strong, say $U/t > 6$, in order to describe the strange metal. We argue that to obtain phenomenologically acceptable underdoped normal state characteristics like T^* , pseudogap values, and spectral weight distribution, a large value of U is detrimental. Surprisingly the resistivity in the above temperature range is linear $\rho = \rho_0 + \alpha \frac{m^*}{e^2 n \hbar} T$ with the "Planckian" coefficient α of order one.

Physical nature of the d-wave pairing in high T_c cuprates remains a hotly debated topic in condensed matter physics. However it was noticed early on that the normal state is as unusual as the superconducting one. The two main unusual features, broadly referred to as the pseudogap[1] and the strange metal [2], cannot be described in the customary framework of the Landau liquid. A pseudogap appears near the antinodal points below temperature T^* and increases in the underdoped regime $p < p_{opt}$ ($p_{opt} = 0.16$) towards the Mott insulator phase reaching values $\Delta = 100 - 200\text{meV}$ [3, 4]. A natural explanation relies on the short range antiferromagnetic (AF) order, since the pseudogap regime borders the Mott insulator phase at very low doping. It was observed[5] that the Fermi surface fractures into small "pockets" for doping below the Lifshitz point p^* precisely when the pseudogap vanishes. This is described quite well by variants of the phenomenological RVB model[6] derived from a Hubbard model with on site repulsion U (and various hopping parameters $t, t' \dots$) within a generalization of the mean field theory largely preserving the quasiparticle picture[7].

The hallmark of the strange metal is linear resistivity in the 100 – 450K temperature range at intermediate and relatively large doping, generally above T^* . It is believed that the quasiparticle picture should be properly modified in this phase. Approaches, like the marginal Fermi liquid[8], quantum criticality[9], and Planckian dissipation[10], explain part of the experimental results, but typically start from Hamiltonians different from those used to describe the pseudogap physics. Thus each particular aspect of the normal state can be captured by a particular phenomenological model to provide a consistent description of the whole normal state (not including superconductivity) phase diagram, see Fig. sm2 in Supplemental Material I (SMI), but a single theory is still a challenge. The main problem seems to be the conflict between two "paradigms". It is widely accepted that *strong* electron correlations (in our case on-site repulsion U larger than the band width of $\sim 5t$) play a central role in both the spin fluctuation theory of the d-wave superconductivity and in the normal state properties. It seems consistent with the measured values of $U \sim 1 - 3\text{eV}$ for the parent material ($x = 0$) Mott gap in many cuprates. First principle derivations (almost exclusively at zero doping) of the "mesoscopic" one band Hamiltonian support a strong coupling[11]. For one layer cuprates, one obtains $U = 7.7t$ for La_2CuO_4 ($T_c = 34\text{K}$ at p_{opt}), $U = 7.2t$ for $\text{HgBa}_2\text{CuO}_4$ ($T_c = 96\text{K}$). The trend upon the inclusion of the long range Coulomb interactions on the microscopic level however is towards lower values[12]: $U = 6.6t$ for La_2CuO_4 , $U = 4.5t$ for $\text{HgBa}_2\text{CuO}_4$. Electron doped and infinite layer cuprates have significantly lower values $U/t = 1.3 - 3$, so that in some cases the Mott insulator phase is missing[13], e.g. Nd_2CuO_4 ($T_c = 24\text{K}$) one obtains [12] $U/t = 2.6$.

Upon doping, the effective coupling strength U in the mesoscopic level is expected to decrease. Recently a first principle study of doped cuprates $\text{La}_{2-p}\text{Sr}_p\text{CuO}_4$, $p = 0.25$, was performed[14]. Although the values of U were not explicitly calculated, reduction of the gap at crystallographic X point by a factor of 2.5 compared to the parent material indicates a lower value. To graphically demonstrate the qualitative distinction between the strongly and intermediate coupling regimes, let's look at the crossover temperature T^* in the simplest Hubbard model at half filling. Interpolating between the early "simplistic" Hartree-Fock (HF) approximation at small coupling and the nonlinear σ model at large coupling [15], one expects a maximum to appear at $U = 5t$, (blue curve in Fig.1). The gaussian perturbation theory[16] at intermediate coupling interpolated with the CDMFT diagrammatic approach[17] at strong coupling gives rise to correction (purple curve in Fig.1). The U dependence of T^* obtained from these two

* hckao@phy.ntnu.edu.tw

† lidp@pku.edu.cn

‡ baruchro@hotmail.com

calculations share the same feature: rising monotonically at intermediate coupling and decreasing at strong coupling. This separates the (Slater) weakly correlated from the (Mott-Heisenberg) strongly correlated domains. It is sometimes referred to [12, 18] as the "Mott-Slater transition". The feature remains intact (with typically lower values of T^*) at nonzero doping.

The high values of the coupling at optimal doping are naturally favoured in the Hubbard model description of both the normal and superconducting states. Recently, however, serious doubts were cast on this possibility. Employing the tensor network [19], constrained path Quantum Monte Carlo (CPQMC), density matrix renormalization group (DMRG) [20] and the strong coupling diagram technique (SCDT) [21] methods, it was demonstrated that the d-wave superconductivity is superseded by other phases at least for $U > 6t$. In the Slater regime the Hubbard model does exhibit d-wave superconductivity within perturbation theory [22], but its T_c is too low. Whether the Hubbard model supports sufficiently strong d-wave superconductivity at intermediate region $2 < U/t < 5$ is still an open question considering recent opposite claims [23, 24]. In addition the coupling strength is poorly correlated with the observed values in cuprates, e.g. the highest $T_c = 133K$ (under ambient conditions) tri-layer superconductor [12] $HgBa_2Ca_2Cu_3O_8$ has DFT estimated (zero doping) value of $U/t = 2.5$ only. To quote the authors, "Our results suggest that the strong correlation enough to induce Mott gap may not be a prerequisite for the high- T_c superconductivity." Recent alternatives include the apical phonon [24] and polaron [25] mechanisms.

A general feature of the strong coupling scenario is that the spectrum is expected to be greatly reconstructed and might not contain well defined quasiparticles. However quasiparticles are observed in numerous experiments perhaps excluding the strange metal regions [26]. The ARPES experiments and transport properties are "phenomenologically" described by the quasiparticle picture thus tacitly assuming a weak coupling. This includes description of small Fermi "pockets" in the underdoped regime, and the Landau liquid in highly overdoped samples [6]. In addition the order of magnitude of the pseudogap (up to 200meV at $p = 0.05$) is smaller than U for strong coupling, thus favoring an intermediate coupling option $U/t \sim 2 - 4$. In this case the quasiparticles are well defined and symmetrized mean field approach [16] may be used to describe the temperature range above 100K and doping above $p = 0.1$. This includes physics of the strange metal and pseudogap for sufficiently large Fermi arcs (pockets).

In this letter the normal state properties of a generic (one layer) hole cuprate (e.g. $HgBa_2CuO_{4+p}$) in the doping ($0.1 < p < 0.3$) and temperature ($100K < T < 460K$) range are described by the one band intermediate coupling Hubbard model. The symmetrization method [16] describing the short range AF state $T < T^*$, is applied to calculate both the spectral weight and conductivity. Surprisingly linear resistivity, $\rho = \rho_0 + AT$, is obtained with A comparing well with experiments [27, 28]. Quantitative comparison of the conductivity with experiments therefore goes beyond scaling arguments [9]. The transition at T^* is comparable to that observed in ARPES [29] or transport. The transport versus spectroscopic T^* determination is discussed within a well defined framework.

The single band Hubbard model is defined by the Hamiltonian:

$$H = \sum_{\mathbf{k}, \alpha=\uparrow, \downarrow} a_{\mathbf{k}}^{\alpha\dagger} (\varepsilon_{\mathbf{k}} - \mu) a_{\mathbf{k}}^{\alpha} + U \sum_{\mathbf{i}} n_{\mathbf{i}}^{\uparrow} n_{\mathbf{i}}^{\downarrow}; \quad (1)$$

$$\varepsilon_{\mathbf{k}} = -2t(\cos k_x + \cos k_y) - 4t' \cos k_x \cos k_y - 2t''(\cos 2k_x + \cos 2k_y).$$

The lattice spacing a is the unit of length. Hoppings up to the third nearest neighbor are included with values $t = 250$ meV, $t' = -0.16t$, $t'' = 0.09t$. The chemical potential μ varies in a wide range and the on-site $U = 2.5t$.

Due to strong fluctuations in 2D, true long-range order exists only for discrete symmetry breaking. Since the model possesses a continuous $SU(2)$ spin symmetry, AF correlations are always short range. Nevertheless, a well-defined crossover temperature T^* exists that separates the short range AF from the paramagnetic phase. At least naively, the symmetry is "almost" broken in the sense that the correlator typically decreases slowly. The gaussian covariant approximation is the simplest variational approach which may account for the (spurious) dynamical symmetry breaking. It is described in details for bosonic and fermionic systems in ref. [30]. In a recent paper [16] we proposed a "symmetrization" method to study strongly interacting electronic systems in the pseudogap phase. Symmetrization is achieved by integration of a one or two body correlator over the almost broken symmetry group. The method was tested on the benchmark models, the 1D and 2D one band Hubbard models.

One starts with a solution of the gaussian equations, paramagnetic or AF [31], ignoring the spiral ones [32]), and corrects it perturbatively by adding the leading self energy correction. The method was originally proposed [33, 34] in the context of bosonic theories and is adapted to the fermionic case in SMI. The correction gives the main contribution to the scattering rate determining the conductivity, see SMII. All the frequency summations are performed exactly, so that no problematic analytic continuation is needed. Full analytic expressions in both the paramagnetic and pseudogap phases are also given. Of course the range of validity of the expansion is limited by the requirement that a high order correction (the order is rigorously defined in ref. [34]) around the gaussian approximation should be smaller than the preceding ones. As an example we present in Fig. sm8 the inverse compressibility of the Hubbard model with $U = 6t$ and $t' = -0.2t$, $t'' = 0$ at sufficiently high temperature, $0.2t < T < 8t$, for doping $0.15 < p < 0.3$. It almost coincides with the recent MC simulation [35] in this range of parameters. For a much smaller coupling $U = 2.5t$ the lower bound of the applicable temperature is expected to extend down to a much lower value, see SMIII.

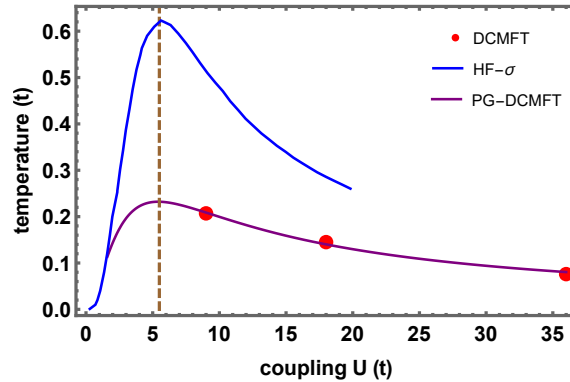


FIG. 1. The crossover temperature T^* in the Hubbard model with ($t' = 0$) at half filling. The blue curve is the HF approximation at small coupling and the nonlinear σ model at large coupling interpolation. The purple curve is the gaussian perturbation theory at intermediate coupling interpolated with the CDMFT diagrammatic approach at strong coupling.

The conductivity (per CuO layer) is calculated by replacing Greens' function in the standard Lindhard formula (derived from the Kubo formula in SMII):

$$\sigma = -\frac{\pi e^2}{\hbar N} \int_{\omega=-\infty}^{\infty} f'_F(\omega) \sum_{\mathbf{k}} v(\mathbf{k})^2 A(\omega, \mathbf{k})^2. \quad (2)$$

Here $f_F[\varepsilon] = (1 + \exp[\varepsilon/T])^{-1}$ is Fermi distribution and the spectral weight is $A(\omega, \mathbf{k}) = -1/\pi \text{Im}[G(\omega, \mathbf{k})]$. The (unrenormalized) Fermi velocity is $v_i(\mathbf{k}) = \frac{1}{\hbar} \frac{\partial \varepsilon_{\mathbf{k}}}{\partial k_i}$. It is important to note that the factor,

$$v(\mathbf{k})^2 = 4 \left\{ (t + 2t' \cos k_y + 4t'' \cos k_x)^2 \sin^2 k_x + (k_x \leftrightarrow k_y) \right\}, \quad (3)$$

vanishes quadratically at the van Hove singularities Gamma and M, see Fig. sm4. As a consequence the anti-node region, the Γ and the M regions practically do not contribute to the conductivity. It is important *not to make* the simplification of replacing the $f'_F[\omega]$ factor in Eq.(2) by a delta function.

We have compared our method with recent MC simulation[35] for $t' = -0.2t$, $t'' = 0$ at relatively high coupling $U = 6t$ with doping $p = 0.15 - 0.3$ and temperatures $T = 0.2t - 8t$. This shows that the postgaussian approximation is still valid for such a large coupling[16]. The resistivity curves are slightly shifted, see Fig. sm9, compared to the MC simulation. Obviously the case is not realistic since the values of T^* determined from nonlinearity of $\rho(T)$ are thousands of Kelvin ($\sim t$ taken as 250 meV) for low doping. Analytically demonstrated [36] linearity in the large $T \gg t$ limit is quite common and is not directly related to the strange metal that appears at temperatures 100–450K which is obviously much lower than the hopping energy t .

To characterize the pseudogap phase and the crossover line T^* , spectral weight, measured in numerous ARPES experiments[37], is calculated. The spectral weight at the Fermi level as a function of quasi-momentum, $A(\omega = 0, \mathbf{k})$ for $p = 0.21$ (calculated at 220K) is given in Fig. 2a. One notes that the spectral weight in the antinodal region is larger than that in the nodal region by a factor of about 2.

In Fig. 2b the spectral weight dependence on frequency across the T^* crossover line for $p = 0.16$ is given. We choose the quasi-momentum $\mathbf{k} = \pi(1, \frac{1}{8})$ close to the Fermi surface, see the magenta blob in Fig. 2a. Several curves for the spectral weight with temperature in the range $T = 100 - 280\text{K}$ are shown. The crossover T^* therefore lies in the temperature range between $T = 260\text{K}$ and 280K . The pseudogap value corresponds to the energy spacing between the two maxima. It widens as the temperature decreases. Simultaneously the peak values become higher and in the valley between them the spectral weight vanishes. These features are qualitatively consistent with ARPES observations[37]. The postgaussian correction modifies the HF picture by shifting T^* to a lower value and reducing the pseudogap value at low temperature. For other quasi-momenta (like near the nodal position given in Fig. sm6) the dependence is similar and in accord with available experiments.

Now let's turn to transport. The DC resistivity (per CuO layer) is given in Fig. 3. It clearly demonstrates the linear dependence, $\rho = \rho_0 + AT$, in the strange metal region of the phase diagram. This is the main result of the present paper. The value of $A \simeq 25 \Omega/\text{K}$ (resistance per layer) at doping $p = 0.16$ are a bit higher than those found by interpolating the $La_{2-p}Sr_pCuO_4$ data of [27] to $p = 0.16$. However, as was discussed in the Introduction, the intermediate value of $U = 2.5t$ is smaller than that of $La_{2-p}Sr_pCuO_4$. We found that for higher value of U , the slope

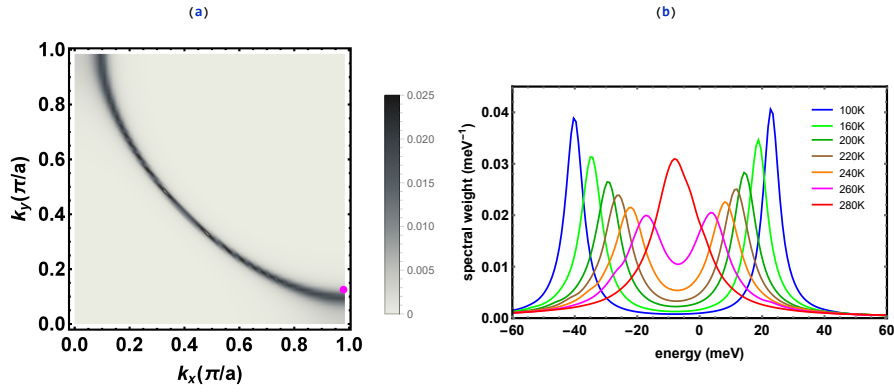


FIG. 2. (a) The zero frequency spectral weight in the first quarter of the Brillouin zone. (b) Closing the pseudogap at a point close to the Fermi surface of (a) (the pink blob) and near the anti-node. Spectral weight as a function of frequency. The paramagnetic phase (a single peak) is represented by $T = 280\text{K}$. The rest are anti-ferromagnetic (a double peak).

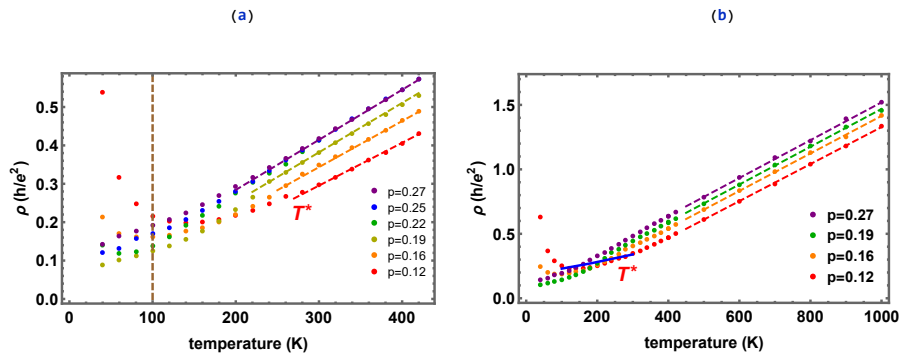


FIG. 3. Resistivity in the strange metal phase. (a) The postgaussian results are very accurate beyond 100K (dashed-brown line). Dashed straight lines are interpolation. The transport determined crossover temperature is marked by T^* . (b) A larger temperature and doping range demonstrate crossover to the Landau liquid.

decreases. Since disorder is always present in cuprates, doping-dependent value of disorder strength $\eta_0 = \hbar/2\tau_0$ must be taken into account. We have chosen a small value of $\eta_0 = 3\text{meV}$. Using a different value of η_0 (see Fig. sm5) would increase the residual resistivity ρ_0 . At higher doping the crossover to Landau liquid appears, see Fig. 3b.

To understand qualitatively the results, we plot the integrand of the imaginary part of the self energy (due to on site repulsion), $\text{Im}(\Sigma_k) = \hbar/2\tau_k$, at $\omega = 0$ as a function of quasi-momentum in Fig. 4a,b for two different temperatures. For this purpose a higher doping $p = 0.26$ is considered and thus there would be no "intercept" ρ_0 in Fig. 3. The lower doping case will be discussed in SMII. Plots of the ratio $A(\mathbf{k})/T$ over the whole BZ for $T = 200\text{K}$, 400K are shown in Fig. 4 and the curves are hardly distinguishable. This demonstrate that $1/2\tau_k \propto T$. Due to the maximum of the factor $v(\mathbf{k})^2$ in Eq. (2) most important contribution to conductivity comes from a broad region near the nodal point. To demonstrate this, we plot the spectral weight dependence along the $\Gamma - M$ line (see the pink line in Fig. 4a) in Fig. 4c. The dependence on location is different for temperatures 200K, 300K, 400K. However, all the three curves almost coincide, when the spectral weight is divided by T , as shown in Fig. 4d. One observes from Fig. 2a that the Fermi surface in this case is nearly circular. Thus the effective mass approximation can be applied to estimate the conductivity via the Drude formula $\sigma = e^2 n \tau / m^*$ with $\hbar/2\tau = \text{Im}[\Sigma_{node}] \simeq 0.25T$. This is close to the result in Fig. 3. Using the phenomenological (Planck) formula $A = \alpha m^* / e^2 n \hbar$ [27], one estimates $\alpha = 0.5$.

To summarize, an intermediate coupling one band Hubbard model can be used to describe the two most important unusual normal state features of cuprates: the pseudogap and strange metal. Both the spectroscopic and transport properties of the cuprates in the whole doping range were considered on the same footing within a relatively simple (symmetrized) postgaussian approximation. It is valid for intermediate couplings $U/t = 1 - 4$ in the temperature range $T = 100 - 500\text{K}$. We have assumed a relatively small coupling that is independent of doping in the range $0.1 - 0.3$. For a smaller doping, especially in the Mott insulator phase, the coupling on the effective tight binding scale increases and a different method would be required. This provides an alternative to the commonly accepted paradigm that the coupling at a significant doping should be strong enough, say $U/t > 6$, for the system to describe the strange metal. We argued (see also description of the Lifshitz transition and fractionalization of the Fermi surface

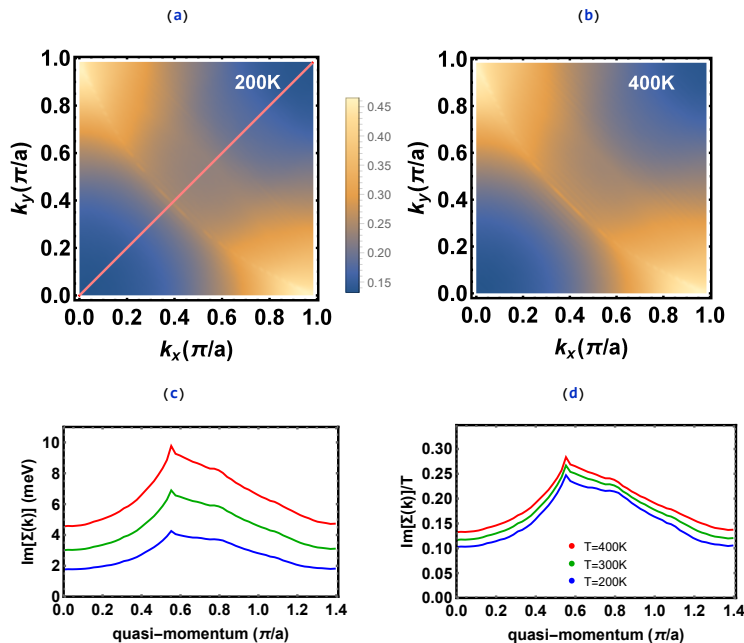


FIG. 4. (a) The self energy due to Hubbard repulsion for doping $p = 0.26$. The imaginary part of the self energy divided by temperature, $\text{Im}[\Sigma(0, \mathbf{k})/T]$, in the first quarter of the BZ for 200K. (b) Same for 400K. Note the maximum on the Fermi surface (shown in Fig. 2a). (c) The imaginary part of the self energy for temperatures at 200K, 300K, and 400K on the Γ to M line (marked by a pink line in (a)). (d) The imaginary part of the self energy divided by temperature for the same temperature.

in a similar framework[24]) that to obtain phenomenologically acceptable underdoped normal state characteristics like T^* , pseudogap values, and spectral weight distribution, a large value of U is detrimental. Of course this applies only to the short range AF order interpretation of the pseudogap. Surprisingly the resistivity in the above temperature range is linear $\rho = \rho_0 + \alpha \frac{m^*}{e^2 n \hbar} T$ with the "Planckian" coefficient $\alpha \sim 0.5$. Interestingly the spectroscopy estimate of T^* (from the vanishing of the pseudogap, Fig. 2b, as observed in ARPES) is typically lower than that determined from resistivity (Fig. 3).

First principle calculations for parent materials of the electron doped cuprates generally result in intermediate or even small values of the effective U [12]. The present study demonstrates that for hole doped cuprates the intermediate coupling option is viable despite the fact that most first principle determinations for *parent materials* favour a large coupling [11]. Materials like La_2CuO_4 , $Bi_2Sr_2CuO_6$ perhaps are really strongly coupled even when doped, but higher T_c superconductors like $HgBa_2CuO_4$, $Tl_2Ba_2CuO_6$ might belong to the intermediate coupling class when doped. The situation with two or three layered cuprates should be similar to the model adapted to include inter-layer hopping.

The authors are very grateful to J. Wang, B. Shapiro, Z. Sun for numerous discussions. We would also like to thank the National Center for High-performance Computing (NCHC) of National Applied Research Laboratories (NARLabs) in Taiwan for providing computational and storage resources. H.C.K and B. R. are supported by MOST-110-2112-M-A49 -012 -MY2 of MOST, Taiwan. D. P. L. was supported by National Natural Science Foundation of China (No. 11674007 and No. 91736208).

-
- [1] S. Hufner, M. A. Hossain, A. Damascelli and G. A. Sawatzky, Rep. Prog. Phys. **71**, 062501 (2008); J. P. Carbotte, T. Timusk and J. Hwang, Rep. Prog. Phys. **74**, 066501 (2011).
[2] B. Keimer, S. A. Kivelson, M. R. Norman, S. Uchida, J. Zaanen, Nature, **518**, 179 (2015).
[3] J.L. Tallon and J.W. Loram, Physica C **349**, 53 (2001); J. L. Tallon, J. G. Storey, J. R. Cooper, and J. W. Loram, Phys. Rev. B **101**, 174512 (2020).
[4] I. M. Vishik et al., Proc. Nat. Acad. Sci. U.S.A. **109**, 18332 (2012); M. Hashimoto, I. M. Vishik, R.-H. He, T. P. Devereaux and Z.-X. Shen, Nat. Phys. **10**, 483 (2014);
[5] S. Benhabib, A. Sacuto, M. Civelli, I. Paul, M. Cazayous, Y. Gallais, M.-A. Méasson, R. D. Zhong, J. Schneeloch, G. D. Gu, D. Colson, and A. Forget, Phys. Rev. Lett., **114**, 147001 (2015).

- [6] K.-Y. Yang, T. M. Rice, and F. C. Zhang, *Phys. Rev.* **B 73**, 174501(2006); T. M. Rice, K.-Y. Yang, and F. C. Zhang, *Rep. Prog. Phys.* **75**, 016502 (2012).
- [7] J. Reiss, D. Rohe, and W. Metzner, *Phys. Rev.* **B 75**, 075110 (2007); Y. Yamaji and M. Imada, *Phys. Rev.* **B 83**, 214522 (2011).
- [8] C. M. Varma, *Phys. Rev.* **B 55**, 14554 (1997); C. M. Varma, *Rev. Mod. Phys.* **92**, 031001 (2020).
- [9] P. Coleman, and A. J. Schofeld, *Quantum criticality.* *Nature* **433**, 226 (2005).
- [10] A. Legros, S. Benhabib, W. Tabis, F. Laliberté, M. Dion, M. Lizaire, B. Vignolle, D. Vignolles, H. Raffy, Z. Z. Li, P. Auban-Senzier, N. Doiron-Leyraud, P. Fournier, D. Colson, L. Taillefer, and C. Proust, *Nature Physics* **15**, 142 (2019).
- [11] F. Nilsson, K. Karlsson, and F. Aryasetiawan, *Phys. Rev.* **B 99**, 075135 (2019).
- [12] S. W. Jang, H. Sakakibara, H. Kino, T. Kotani, K. Kuroki, and M. J. Han, *Sci. Rep.* **6**, 33397 (2016).
- [13] J. Hea, C. R. Rotundua, M. S. Scheurerd, Y. Hea, M. Hashimoto, K.-J. Xu, Y. Wang, E. W. Huang, T. Jia, S. Chen, B. Moritz, D. Lue, Y. S. Lee, T. P. Devereaux, and Z.-X. Shen, *PNAS* **116**, 3449 (2019).
- [14] J. W. Furness, Y. Zhang, C. Lane, I. Gianina Buda, B. Barbiellini, R. S. Markiewicz, A. Bansil, J. Sun, *Commun. Phys.* **1**, 11 (2018).
- [15] K. Borejsza and N. Dupuis, *EPL* **63**, 722 (2003).
- [16] B. Rosenstein, D. Li, T. X. Ma and H.C. Kao, *Phys. Rev.* **B 100**, 125140 (2019).
- [17] A. Reymbaut, S. Bergeron, R. Garioud, M. Thenault, M. Charlebois, P. Semon, and A.-M. S. Tremblay, *Phys. Rev. Research* **1**, 023015 (2019).
- [18] R. S. Markiewicz, I.G. Buda, P. Mistark, C. Lane, and A. Bansil, *Sci. Rep.* **7**, 44008 (2017).
- [19] B.-X. Zheng, C.-M. Chung, P. Corboz, G. Ehlers, M.-P. Qin, R. M. Noack, H. Shi, S. R. White, S. Zhang, and G. K.-L. Chan, *Science* **358**, 1155 (2017); K. Ido, T. Ohgoe, and M. Imada, *Phys. Rev.* **B 97**, 045138 (2018).
- [20] H.-C. Jiang, and T. P. Devereaux, *Science* **365**, 1424 (2019); M. Qin, C.-M. Chung, H. Shi, E. Vitali, C. Hubig, U. Schollwöck, S. R. White, and S. Zhang, *Phys. Rev.* **X 10**, 031016 (2020).
- [21] R. E. I. Sherman, *Phys. Scr.* **96**, 095804 (2021).
- [22] S. Raghu, S. A. Kivelson, and D. J. Scalapino, *Phys. Rev.* **B 81**, 224505 (2010).
- [23] F. Šimkovic, Y. Deng, and E. Kozik, *Phys. Rev.* **B 104**, L020507 (2021).
- [24] B. Rosenstein and B. Ya. Shapiro, *J. Phys. Commun.* **5**, 055013 (2021).
- [25] S. Dzhumanov, "Microscopic theory of pseudogap phenomena and unconventional Bose-liquid superconductivity and superfluidity in high-Tc cuprates and other systems", arXiv:1912.12407v5 [cond-mat.supr-con] (2020) and references therein.
- [26] S.-D. Chen, M. Hashimoto, Y. He, D. Song, K.-J. Xu, J.-F. He, T. P. Devereaux, H. Eisaki, D.-H. Lu, J. Zaanen, Z.-X. Shen, *Science* **366**, 1099 (2019).
- [27] A. Legros, S. Benhabib, W. Tabis, F. Laliberté, M. Dion, M. Lizaire, B. Vignolle, D. Vignolles, H. Raffy, Z. Z. Li, P. Auban-Senzier, N. Doiron-Leyraud, P. Fournier, D. Colson, L. Taillefer, and C. Proust, *Nat. Phys.* **15**, 142 (2019).
- [28] C. Putzke, S. Benhabib, W. Tabis, J. Ayres, Z. Wang, L. Malone, S. Licciardello, J. Lu, T. Kondo, T. Takeuchi, N. E. Hussey, J. R. Cooper, and A. Carrington, *Nat. Phys.* **17**, 826 (2021).
- [29] M. K. Chan, C.J. Dorow, L. Mangin-Thro, Y. Tang, Y. Ge, M. J. Veit, G. Yu, X. Zhao, A.D. Christianson, J.T. Park, Y. Sidis, P. Steffens, D.L. Abernathy, P. Bourges, and M. Greven, *Nat. Com.* **7**, 10819 (2016).
- [30] J. F. Wang, D. P. Li, H. C. Kao, and B. Rosenstein, *Ann. Phys.* **380**, 228 (2017); B. Rosenstein and A. Kovner, *Phys. Rev.* **D 40**, 523 (1989); B. Rosenstein and D. Li, *Phys. Rev.* **B 98**, 155126 (2018).
- [31] J. E. Hirsch, *Phys. Rev.* **B 31**, 4403 (1985); H. Q. Lin, and J. E. Hirsch, *Phys. Rev.* **B 35**, 3359 (1987).
- [32] M. A. Timirgazin, P. A. Igoshev, A. K. Arzhnikov. V. Yu. Irkhin, *J. Low Temp. Phys.* **185**, 651 (2016).
- [33] Ruggeri, G. J., and D. J. Thouless, *J. Phys. F: Met. Phys.* **6**, 2063 (1976).
- [34] B. Rosenstein and D. Li, *Rev. Mod. Phys.* **82**, 107 (2010).
- [35] E. W. Huang, R. Sheppard, B. Moritz, T. P. Devereaux, *Science* **366**, 987 (2019).
- [36] J. Kokalj, *Phys. Rev.* **B 95**, 041110 (2017); C. H. Mousatov, I. Esterlis, S. A. Hartnoll, *Phys. Rev. Lett.* **122**, 186601 (2019).
- [37] I. M. Vishik, N. Barisic, M. K. Chan, Y. Li, D. D. Xia, G. Yu, X. Zhao, W. S. Lee, W. Meevasana, T. P. Devereaux, M. Greven, and Z.-X. Shen, *Phys. Rev.* **B 89**, 195141 (2014); Y.-G. Zhong, J.-Y. Guan, X. Shi, J. Zhao, Z.-C. Rao, C.-Y. Tang, H.-J. Liu, Z. Y. Weng, Z. Q. Wang, G. D. Gu, T. Qian, Y.-J. Sun, and H. Ding, *Phys. Rev.* **B 98**, 140507(R) (2018); I. M. Vishik, *Rep. Prog. Phys.* **81**, 062501 (2018).